Jyväskylän yliopiston julkaisuarkisto
Jyväskylä University Digital Archive

UNIVERSITY OF JYVÄSKYLÄ

This is an electronic reprint of the original article.
This reprint *may differ* from the original in pagination and typographic detail.

Author(s): ALICE Collaboration

Title: Longitudinal asymmetry and its effect on pseudorapidity distributions in Pb–Pb collisions at √sNN = 2.76 TeV

Year: 2018

Version:

Please cite the original version:

ALICE Collaboration. (2018). Longitudinal asymmetry and its effect on pseudorapidity distributions in Pb–Pb collisions at √sNN = 2.76 TeV. Physics Letters B, 781, 20-32. https://doi.org/10.1016/j.physletb.2018.03.051

All material supplied via JYX is protected by copyright and other intellectual property rights, and duplication or sale of all or part of any of the repository collections is not permitted, except that material may be duplicated by you for your research use or educational purposes in electronic or print form. You must obtain permission for any other use. Electronic or print copies may not be offered, whether for sale or otherwise to anyone who is not an authorised user.

Physics Letters B 781 (2018) 20–32

Contents lists available at ScienceDirect

Physics Letters B

www.elsevier.com/locate/physletb

Longitudinal asymmetry and its effect on pseudorapidity distributions in Pb–Pb collisions at $\sqrt{s_{NN}} = 2.76$ TeV

ALICE Collaboration *

ARTICLE INFO

Article history:
Received 30 October 2017
Received in revised form 9 March 2018
Accepted 15 March 2018
Available online 22 March 2018
Editor: L. Rolandi

ABSTRACT

First results on the longitudinal asymmetry and its effect on the pseudorapidity distributions in Pb–Pb collisions at $\sqrt{s_{NN}} = 2.76$ TeV at the Large Hadron Collider are obtained with the ALICE detector. The longitudinal asymmetry arises because of an unequal number of participating nucleons from the two colliding nuclei, and is estimated for each event by measuring the energy in the forward neutron-Zero-Degree-Calorimeters (ZNs). The effect of the longitudinal asymmetry is measured on the pseudorapidity distributions of charged particles in the regions $|\eta| < 0.9$, $2.8 < \eta < 5.1$ and $-3.7 < \eta < -1.7$ by taking the ratio of the pseudorapidity distributions from events corresponding to different regions of asymmetry. The coefficients of a polynomial fit to the ratio characterise the effect of the asymmetry. A Monte Carlo simulation using a Glauber model for the colliding nuclei is tuned to reproduce the spectrum in the ZNs and provides a relation between the measurable longitudinal asymmetry and the shift in the rapidity (y_0) of the participant zone formed by the unequal number of participating nucleons. The dependence of the coefficient of the linear term in the polynomial expansion, c_1, on the mean value of y_0 is investigated.

© 2018 The Author(s). Published by Elsevier B.V. This is an open access article under the CC BY license (http://creativecommons.org/licenses/by/4.0/). Funded by SCOAP[3].

1. Introduction

In a heavy-ion collision, the number of nucleons participating from each of the two colliding nuclei is finite, and will fluctuate event-by-event. The kinematic centre of mass of the participant zone, defined as the overlap region of the colliding nuclei, in general has a finite momentum in the nucleon–nucleon centre of mass frame because of the unequal number of nucleons participating from the two nuclei. This momentum causes a longitudinal asymmetry in the collision and corresponds to a shift of rapidity of the participant zone with respect to the nucleon–nucleon centre of mass (CM) rapidity, termed the rapidity-shift y_0. The value of y_0 is indicative of the magnitude of the longitudinal asymmetry of the collision [1,2]. Assuming the number of nucleons participating from each of the two nuclei is A and B, the longitudinal asymmetry in participants is defined as $\alpha_{\text{part}} = \frac{A-B}{A+B}$ and the rapidity-shift can be approximated as $y_0 \cong \frac{1}{2} ln \frac{A}{B}$ at LHC energies [2].

The shift in the CM frame of the participant zone, which evolves into a state of dense nuclear matter, needs to be explored in heavy-ion collision models. Comparison of model predictions with the observed Λ-polarisation, possibly due to vorticity from the initial state angular momentum surviving the evolution, requires a precise determination of initial conditions and hence the shift in the CM frame [3–5]. Such a shift may also affect observations on correlations amongst particles, which eventually provide information about the state of the matter through model comparisons. Further, the resultant decrease in the CM energy may affect various observables including the particle multiplicity. The transverse spectra are known to be affected by the initial geometry of the events, as estimated through techniques of event shape engineering, indicating an interplay between radial and transverse flow [6]. The measurement of longitudinal asymmetry will provide a new parameter towards event shape engineering, affecting many other observables.

The simplest of all possible investigations into the effect of longitudinal asymmetry is a search for modification of the kinematic distribution of the particles. The pseudorapidity distribution ($dN/d\eta$) of soft particles, averaged over a large number of events, is symmetric in collisions of identical nuclei. These distributions were observed to be asymmetric in collisions of unequal nuclei such as d–Au [7] and p–Pb [8–10] and have been explained in terms of the rapidity-shift of the participant zone [11]. In a heavy-ion collision, the effect of the rapidity-shift of the participant zone should be discernible in the distribution of produced particles. This small effect can be estimated by taking the ratio of pseudorapidity distributions in events corresponding to different longitudinal asymmetries [2].

It was suggested that the rapidity distribution of an event, scaled by the average rapidity distribution, can be expanded in terms of Chebyshev polynomials, where the coefficients of expan-

* *E-mail address:* alice-publications@cern.ch.

https://doi.org/10.1016/j.physletb.2018.03.051
0370-2693/© 2018 The Author(s). Published by Elsevier B.V. This is an open access article under the CC BY license (http://creativecommons.org/licenses/by/4.0/). Funded by SCOAP[3].

sion are measures of the strength of longitudinal fluctuations and can be determined by measuring the two particle correlation function [12]. Using the same methodology, the event-by-event pseudorapidity distributions are also expanded in terms of Legendre polynomials [13]. The ATLAS Collaboration expanded the pseudorapidity distributions in terms of Legendre polynomials and obtained the coefficients by studying pseudorapidity correlations [14].

In the present work, the events are classified according to the asymmetry determined from the measurement of energies of neutron spectators on both sides of the collision [2]. The effect of asymmetry is investigated by taking the ratio of the measured raw $\mathrm{d}N/\mathrm{d}\eta$ distributions for events from different regions of the distribution of measured asymmetry. A major advantage of studying this ratio is the cancellation of (i) systematic uncertainties and (ii) the effects of short range correlations. The first measurements of the effect of asymmetry on the raw $\mathrm{d}N/\mathrm{d}\eta$ distributions are reported here.

The paper is organised as follows: Sect. 2 provides an introduction to the experimental setup and the details of the data sample. Section 3 discusses the characterisation of the change in raw $\mathrm{d}N/\mathrm{d}\eta$ distributions for events classified in different asymmetry regions. Section 4 describes the simulations employed to provide a relation between the measured asymmetry and the rapidity-shift y_0 of the participant zone. The relation between the parameter characterising the change in raw $\mathrm{d}N/\mathrm{d}\eta$ distributions is shown for different centralities in Sect. 5, along with its relation to the estimated values of y_0.

2. Experimental details and data sample

The analysis uses data from Pb–Pb collision events at $\sqrt{s_{\mathrm{NN}}} =$ 2.76 TeV, recorded in the ALICE experiment in 2010, with a minimum bias trigger [15,16]. The data used in the present analysis is recorded in the neutron Zero Degree Calorimeters (ZNs), the V0 detectors, the Time Projection Chamber (TPC) and the Inner Tracking System (ITS). Both ZNs and V0 detectors are on either side of the interaction vertex, those in the direction of positive pseudorapidity axis are referred as V0A and ZNA and those in the opposite direction are referred as V0C and ZNC. A detailed description of the ALICE detectors and their performance can be found elsewhere [17, 18].

The event asymmetry is estimated using the energy measured in the two ZNs situated 114 metres away from the nominal interaction point (IP) on either side. The ZNs detect only spectator neutrons that are not bound in nuclear fragments, since the latter are bent away by the magnetic field of the LHC separation dipole. The ZN detection probability for neutrons is 97.0% ± 0.2% (stat) ±3% (syst) [19]. The relative energy resolution of the $1n$ peak at 1.38 TeV is 21% for the ZNA and 20% for the ZNC [19]. The production of nuclear fragments increases with collision impact parameter degrading the resolution on the number of participating nucleons. The energy in the ZNs is a good measure of the number of spectator neutrons only for the more central collisions [18]. The analysis is limited to the top 35% most central sample and employs data from ∼2.7 million events.

The raw $\mathrm{d}N/\mathrm{d}\eta$ distributions in the region $|\eta| < 0.9$ are obtained by reconstructing the charged particle tracks using the TPC and ITS. The requirements on the reconstructed tracks obtained using the measurements in these detectors are the same as in other earlier analyses [15]. The measured amplitudes in the V0A ($+2.8 < \eta < +5.1$) and V0C ($-3.7 < \eta < -1.7$) are used to estimate the raw $\mathrm{d}N/\mathrm{d}\eta$ distributions of charged particles in the forward regions. Both V0A and V0C are scintillator counters, each with four segments in pseudorapidity and eight segments in azimuth. The raw distributions measured are termed as $\mathrm{d}N/\mathrm{d}\eta$ distributions throughout the manuscript. In order to ensure a uniform detector performance, the present analysis uses events with z position (along the beam direction) of the interaction vertex, V_z, within ± 5 cm of the IP in ALICE. The centrality of Pb–Pb collisions was estimated by two independent methods. One estimate was based on the charged particle multiplicity reconstructed in the TPC and the other was based on the amplitudes in the V0 detectors [20].

3. Analysis and systematic uncertainties

In the present analysis, changes in the raw pseudorapidity distribution of charged particles are investigated for different values of measured asymmetry of the event. The method of measurement of the asymmetry and the parameters characterising the change in $\mathrm{d}N/\mathrm{d}\eta$ distributions are discussed in this section.

3.1. Analysis

Any event asymmetry due to unequal number of nucleons from the two participating nuclei may manifest itself in the longitudinal distributions, i.e. $\mathrm{d}N/\mathrm{d}y$ (or $\mathrm{d}N/\mathrm{d}\eta$) of the produced particles because of a shift in the effective CM. Assuming that the rapidity distributions can be described by a symmetric function about a mean y_0 ($y_0 = 0.0$ for symmetric events), the ratio of the distributions for asymmetric and symmetric events may be written as

$$\frac{(\mathrm{d}N/\mathrm{d}y)_{\mathrm{asym}}}{(\mathrm{d}N/\mathrm{d}y)_{\mathrm{sym}}} = \frac{f(y-y_0)}{f(y)} \propto \sum_{n=0}^{\infty} c_n(y_0)y^n \tag{1}$$

For any functional form of the rapidity distribution, this ratio may be expanded in a Taylor series. The coefficients c_{n} of the different terms in the expansion depend on the shape and the parameters of the rapidity distribution [2]. In the ALICE experiment, the pseudorapidities of the emitted particles were measured. The effect of a rapidity-shift y_0 on the pseudorapidity distribution is discussed in Sect. 4.2.

The unequal number of participating nucleons will yield a nonzero y_0 of the participant zone and will cause an asymmetry in the number of spectators. This asymmetry can provide information about the mean values of y_0 using the response matrix discussed in Sect. 4. The asymmetry of each event is estimated by measuring the energy in the ZNs on both sides of the interaction vertex: E_{ZNA} on the side referred to as the A-side ($\eta > 0$) and E_{ZNC} on the side referred to as the C-side ($\eta < 0$). A small difference in the mean and the relative energy resolution of the $1n$ peak at 1.38 TeV was observed in the performance of the two ZNs [19]. For each centrality interval, the energy distribution in each ZN is divided by its mean, and the width of the $E_{\mathrm{ZNC}}/\langle E_{\mathrm{ZNC}}\rangle$ distribution is scaled to the width of the corresponding distribution using E_{ZNA}. The asymmetry in ZN is defined as

$$\alpha_{\mathrm{ZN}} = \frac{\varepsilon_{\mathrm{ZNA}} - \varepsilon_{\mathrm{ZNC}}}{\varepsilon_{\mathrm{ZNA}} + \varepsilon_{\mathrm{ZNC}}} \tag{2}$$

where $\varepsilon_{\mathrm{ZNC(A)}}$ is a dimensionless quantity for each event, obtained after scaling the distributions of $E_{\mathrm{ZNC(A)}}$ as described above.

For the 15–20% centrality interval, Fig. 1 shows the distribution of the asymmetry α_{ZN}. To investigate the significance of this distribution, the contribution of the resolution of ZNs to the resolution of the asymmetry parameter α_{ZN} is evaluated. For each centrality interval, values of E_{ZNC} and E_{ZNA} are simulated for each event by assuming a normal distribution peaked at the mean value

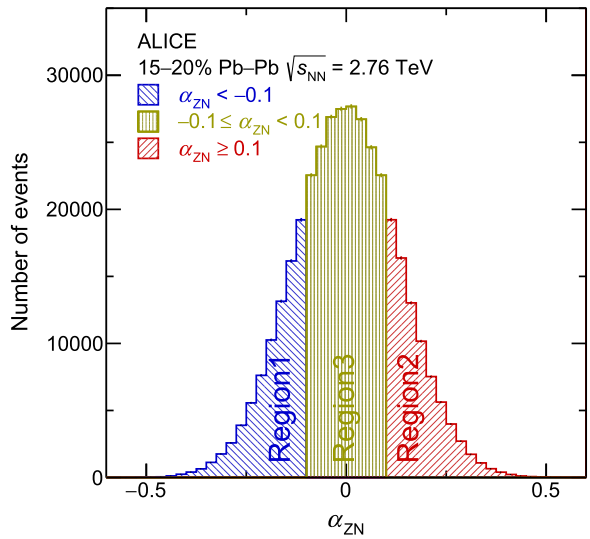

Fig. 1. The distribution of the asymmetry parameter α_{ZN} for the 15–20% centrality interval. The distribution is demarcated into three regions using $|\alpha_{ZN}^{cut}|$. A Gaussian fit to the distribution yields a width of 0.13.

corresponding to the average number of neutrons and the corresponding energy resolution. The average number of neutrons is estimated by dividing the experimental distribution of energy in ZN by 1.38 TeV. These values are used to obtain α_{ZN} for each event and its distribution. The width of the distribution corresponds to the intrinsic resolution of the measured parameter α_{ZN} and varies from 0.023 to 0.050 from the most peripheral (30–35%) selection to the most central (0–5%) selection. The observed width of 0.13 of the distribution of α_{ZN} reported in Fig. 1 is considerably larger than the resolution of α_{ZN} (0.027 for the centrality interval corresponding to the data in the figure) and the increase in width may be attributed to the event-by-event fluctuations in the number of neutrons detected in each ZN. To investigate the effect of α_{ZN} on the $dN/d\eta$ distributions, the events are demarcated into three regions of asymmetry by choosing a cut value α_{ZN}^{cut}. These regions correspond to (i) $\alpha_{ZN} < -\alpha_{ZN}^{cut}$ (Region 1), (ii) $\alpha_{ZN} \ge \alpha_{ZN}^{cut}$ (Region 2) and (iii) $-\alpha_{ZN}^{cut} \le \alpha_{ZN} < \alpha_{ZN}^{cut}$ (Region 3). Regions 1 and 2 are referred to as the asymmetric regions and Region 3 is referred to as the symmetric region.

The effect of the measured asymmetry α_{ZN} on the pseudorapidity distributions is investigated by studying the ratio of $dN/d\eta$ distribution in events from the asymmetric region to those from the symmetric region. There are small differences in the distributions of centrality and vertex position in events of different regions of asymmetry. It is necessary to ensure that any correlation between the ratio of $dN/d\eta$ and the asymmetry is not due to a systematic effect of a shift in the interaction vertex. To eliminate any possible systematic bias on the measured distributions, the $dN/d\eta$ distributions are corrected by weight factors obtained by normalising the number of events in asymmetric and symmetric regions in each 1% centrality interval and each 1 cm range of vertex positions.

For the 15–20% centrality interval, the distributions of these factors in the two cases corresponding to the asymmetry regions 1 and 2 have a mean of 1.0 and an rms of 0.05 and 0.06 respectively. The weight factors do not show any systematic dependence on the position of the vertex. This is expected considering the large distance between the ZNs as compared to variations in the vertex position. The factors show a systematic dependence on 1% centrality bins within each centrality interval. The 1% centrality bin with the greater number of participants tends to have more asymmetric events, presumably to compensate for the decrease in the effective CM energy due to the motion of the participant zone; the weight factor is 1.08 for the most central 15–16% centrality bin and is 0.94 for the 19–20% centrality bin.

The ratio of $dN/d\eta$ for events corresponding to different regions of asymmetry, as shown in Fig. 1, is determined. For $|\eta| < 1.0$, the ratio is obtained using $dN/d\eta$ for tracks. For $|\eta| > 1.0$, the ratio shown in Fig. 2 (a) and (b) is obtained from amplitudes measured in V0A and the one shown in Fig. 2(c) and (d) is from amplitudes measured in V0C. The squares in Fig. 2 (a) and (c) represent the ratio of $dN/d\eta$ in the asymmetry Region 1 to that in Region 3 (R13), and the stars represent the corresponding ratio in Region 2 to Region 3 (R23). The filled circles in Fig. 2 (b) and (d) are obtained by (i) reflecting the data points labelled R23 across $\eta = 0$ and (ii) taking the averages of R13 and reflected-R23 for $|\eta| < 1.0$. A third order polynomial is fitted to the points and the values of the coefficients c_n along with the χ^2 are shown. The polynomial fit to the ratio of $dN/d\eta$ distribution has a dominantly linear term. A small residual detector effect is observed when determining c_1 using data measured in V0A and when using data measured in V0C. In all subsequent discussion, the values of c_1 quoted are the mean of values obtained from the measurements in V0A and V0C.

Considering that the event samples corresponding to different regions of asymmetry are identical in all aspects other than their values of measured α_{ZN}, the observation of non-zero values of c_1 can be attributed to the asymmetry. For a fixed centrality interval, c_1 depends on the choice of α_{ZN}^{cut}. The analysis is repeated for different values of α_{ZN}^{cut} and the dependence of c_1 on α_{ZN}^{cut} is shown in Fig. 3, for different centralities. For each centrality interval the coefficient c_1 has a linear dependence on α_{ZN}^{cut} and the slope increases with decreasing centrality; c_1 increases for events corresponding to larger values of average event asymmetry. The range of values of α_{ZN}^{cut} was guided by the resolution and the width of the distribution of α_{ZN}, as mentioned in reference to Fig. 1. Increasing the value of α_{ZN}^{cut} increases the mean $\langle\alpha_{ZN}\rangle$ for events from the asymmetric class (Region 1 or Region 2), and increases the RMS of α_{ZN} for events from the symmetric class (Region 3).

3.2. Systematic uncertainties

The current method of analysis uses the ratio of two $dN/d\eta$ distributions from events divided on the basis of measurements in ZNs, within a centrality interval. All effects due to limited efficiency, acceptance or contamination would cancel while obtaining the value of the ratio. The contributions to the systematic uncertainties on c_1 are estimated due to the following sources:

1. Centrality selection: the ratio of $dN/d\eta$ is obtained from the measurements of tracks in the ITS+TPC at midrapidity and charge particle signal amplitudes in the V0 at forward rapidities. For the former, the event centrality is determined using the measurements in the V0 and for the latter using the track multiplicity in the TPC. The analysis is repeated by interchanging the centrality criteria and the resultant change in the values of c_1 for different centrality intervals is in the range 0.1% to 3.6%.
2. V0A and V0C: the systematic uncertainty on the mean value of c_1 is estimated by assuming a uniform probability distribution for the correct value of c_1 to lie between the two values obtained using the charged-particle signal amplitudes measured in the V0A and the V0C. The uncertainty is in the range 2.1% to 4.6% and does not depend on the centrality value.
3. Vertex position: the analysis is repeated for the z position of the interaction vertex $|V_z| \le 3.0$ cm. For the most central interval, the results change by less than 0.1%. For the 15–20%

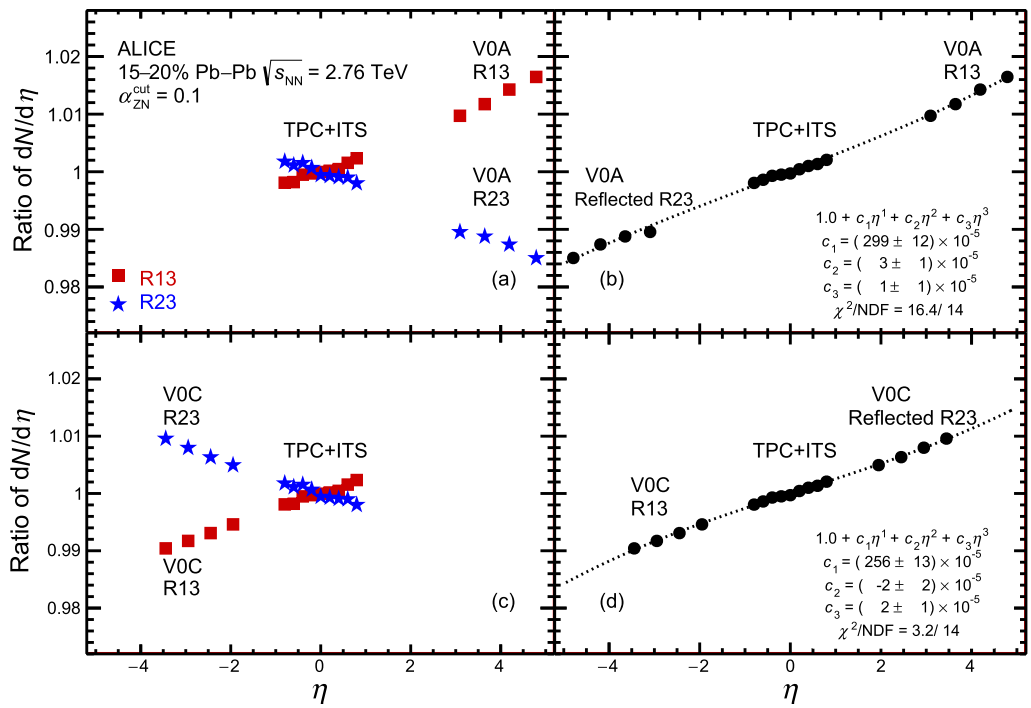

Fig. 2. The ratio of $dN/d\eta$ distribution for events from the different regions of α_{ZN} distribution of Fig. 1. The $dN/d\eta$ distributions are obtained as described in Sect. 2. (a) The square (star) symbols corresponding to R13 (R23) are obtained by taking the ratio of $dN/d\eta$ of events from Region 1 (Region 2) to Region 3. (b) The data points are obtained after reflection across $\eta = 0$ as described in the text. The data for $|\eta| > 1.0$ in panels (a) and (b) are from measurements in V0A and in panels (c) and (d) are from measurements in V0C.

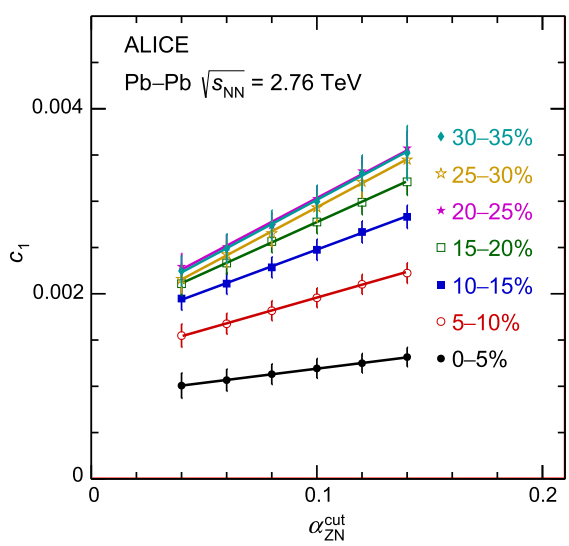

Fig. 3. The coefficient c_1 characterising the change in $dN/d\eta$ distribution for asymmetric regions is shown for different values of α_{ZN}^{cut} (α_{ZN}^{cut} demarcates the asymmetric and symmetric events) for each centrality interval.

centrality interval, the results change by 3.3% and for all other centrality intervals, the changes are less than 1.3%.

4. Weight factors for normalisation: the analysis is also repeated without the weight factors mentioned in Sect. 3.1 for the centrality and the vertex normalisation in the number of events. The change in the results is 4.9% in the most central class and less than 1% for all other centrality intervals.

The total systematic uncertainty is obtained by adding the four uncertainties in quadrature. The resultant uncertainty is in the range 2.3% to 5.8% and is shown by the band in Fig. 8.

4. Simulations

The simulation used for obtaining a relation between rapidity-shift y_0 and the measurable asymmetry α_{ZN} is described in this section. This simulation has three components: (i) a Glauber Monte Carlo to generate number of participants and spectator protons and neutrons, (ii) a function parametrised to fit the average loss of spectator neutrons due to spectator fragmentation (the loss of spectator neutrons in each event is smeared around this average) and (iii) the response of the ZN to single neutrons. The simulation encompassing the above is referred to in the present work as Tuned Glauber Monte Carlo (TGMC), and reproduces the energy distributions in the ZNs. The effect of y_0 on the pseudorapidity distributions has been estimated using additional simulations for a Gaussian dN/dy and are also described in this section.

4.1. Asymmetry and rapidity-shift

The Glauber Monte Carlo model [21] used in the present work assumes a nucleon–nucleon interaction cross section of 64 mb at $\sqrt{s_{NN}}$ = 2.76 TeV. The model yields the number of participating nucleons in the overlap zone from each of the colliding nuclei. The range of impact parameters for each 5% centrality interval is taken from our Pb–Pb centrality paper [20]. For each centrality interval, 0.4 million events are generated.

For each generated event, the number of participating protons and neutrons is obtained, enabling a determination of the rapidity-shift y_0 and the various longitudinal asymmetries. If A and B are the number of spectators (spectator neutrons) in the two colliding nuclei, the asymmetry is referred to as α_{spec} ($\alpha_{spec-neut}$). Fig. 4 (a) shows the correspondence between y_0 and α_{part}. Figs. 4 (b) and (c) show the relation between y_0 and α_{spec} and $\alpha_{spec-neut}$ respectively [2]. These figures show that the rapidity-shift y_0 can be estimated by measuring α_{spec} or $\alpha_{spec-neut}$ in any experiment that uses Zero Degree Calorimeters. However, the lack of information

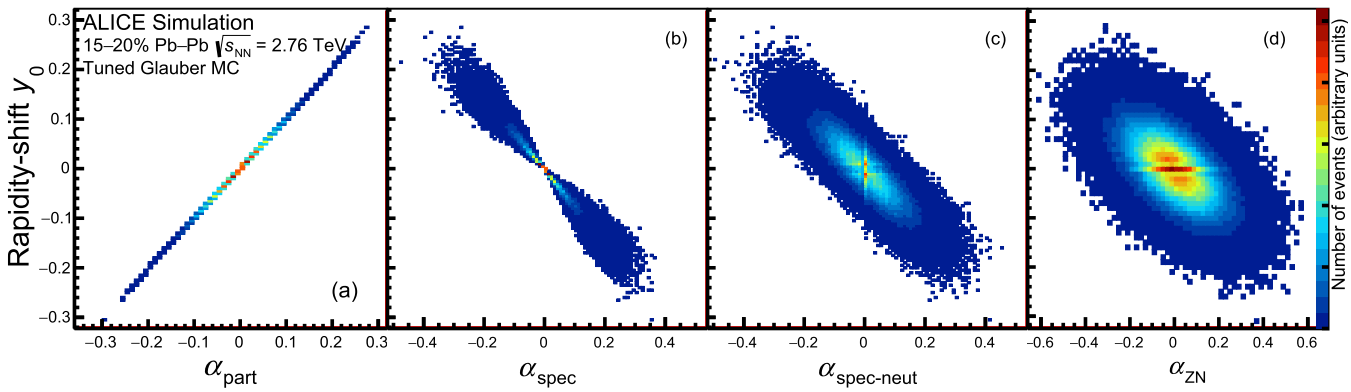

Fig. 4. Rapidity-shift y_0 as a function of asymmetry in (a) number of participants, (b) number of spectators, (c) number of spectator neutrons and (d) energy in ZN obtained using TGMC as described in the text. The results in all four panels are shown for the 15–20% centrality interval.

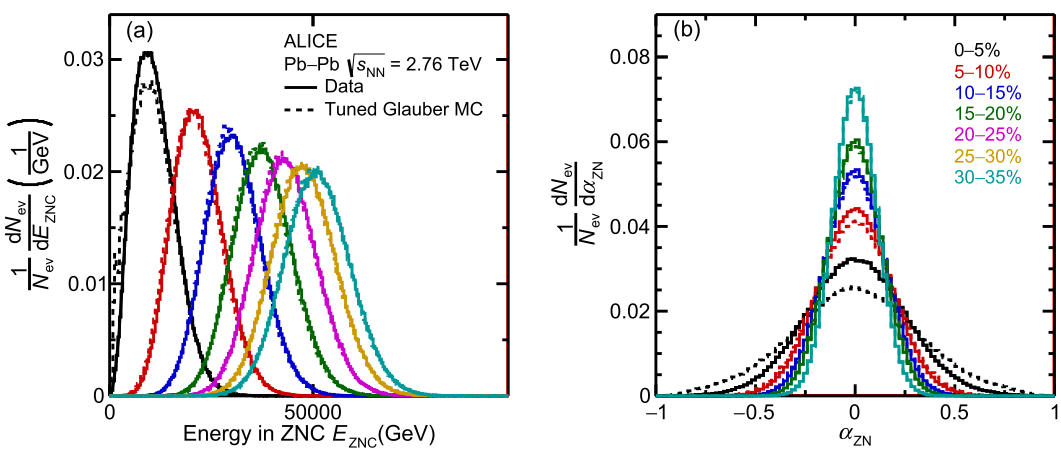

Fig. 5. (a) Distribution of energy in ZNC in each 5% centrality interval for events simulated using TGMC and for the experimental data. The peak of the distribution shifts to smaller values of E_{ZNC} with increasing centrality. (b) Distribution of the asymmetry parameter α_{ZN} in the simulated events and in experimental data for different centralities. The width of the distribution increases with increasing centrality. For clarity, only 5 distributions are shown. The distributions corresponding to 20–25% and 25–30% lie between those of 15–20% and 30–35%.

on the number of participants worsens the precision in determining y_0. Fig. 4 (d) shows the relation between y_0 and α_{ZN} obtained in TGMC, as described in the next paragraph.

The Glauber Monte Carlo is tuned to describe the experimental distributions of ZN energy. For each 1% centrality interval, the mean number of spectator neutrons (N_s) is obtained in the Glauber Monte Carlo. Folding the ZN response yields the simulated values of mean energy as a function of centrality. The experimentally measured mean energy in the ZN is also determined for each 1% centrality interval. The ratio of the measured value of mean energy to the simulated value of mean energy gives the fractional loss (f) of neutrons due to spectator fragments that veer away due to the magnetic field. The value of f for the 0–5% centrality interval is 0.19. For all other centralities it varies from 0.40 for 5–10% to 0.55 for 30–35% centrality interval. A fluctuation proportional to the number of remaining neutrons ($N_s \times (1-f)$) is incorporated to reproduce the experimental distribution of the energy deposited in the ZN shown in Fig. 5 (a). The peak and the RMS of the energy distributions match well. The fractional difference in the position of the peak varies between 3.7% for the 0–5% centrality interval and 0.1% for the 30–35% centrality interval. The fractional difference in RMS for the most central class is 8.6% and is in the range 1.0–2.0% for all other centrality intervals. The distributions of the asymmetry parameter for the TGMC events and the measured data for each centrality interval are shown in Fig. 5 (b). The TGMC contains information of y_0 and α_{ZN} for each event. A scatter plot between y_0 and α_{ZN} is shown in Fig. 4 (d) for the 15–20% centrality interval. This constitutes the response matrix. For any measured value of α_{ZN}, the distribution of y_0 can be obtained. Any difference in the experimental and TGMC distributions of α_{ZN} can be accounted for by scaling the y_0 distribution by the ratio of number of events in data to the number in TGMC as

$$f(y_0, \alpha_{ZN}^{Data}) = f(y_0, \alpha_{ZN}^{TGMC}) \frac{N_{events}^{Data}}{N_{events}^{TGMC}}, \tag{3}$$

with Data (TGMC) in the superscript of number of events, N_{events}, denoting the experimental data (TGMC events). For each of the three regions of asymmetry shown in Fig. 1, corresponding to a chosen value of $\alpha_{ZN}^{cut} = 0.1$, the distribution of rapidity-shift y_0 obtained using the response matrix is shown in Fig. 6. It is worth mentioning that the width of the distribution of y_0 for events from Region 3, corresponding to $-\alpha_{ZN}^{cut} \le \alpha_{ZN} < \alpha_{ZN}^{cut}$, is comparable to the widths of the corresponding distributions from Regions 1 and 2. The effect of difference in the value of the means of the y_0 distributions is investigated in the present work.

4.2. Effect of rapidity-shift on pseudorapidity distributions

The effect of a shift in the rapidity distribution by y_0 on the measurable pseudorapidity distribution ($dN/d\eta$) is investigated using simulations. For each event, the rapidity of charged particles is

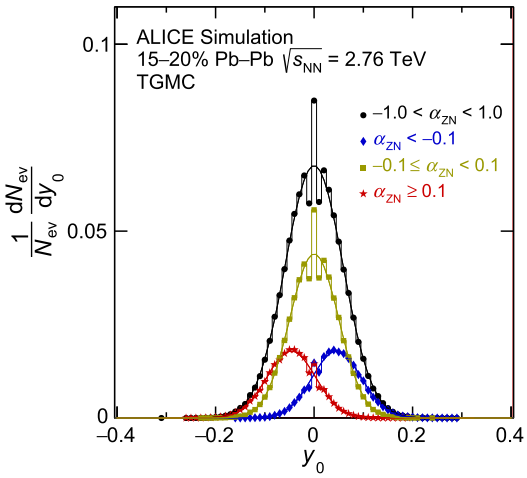

Fig. 6. The distribution of rapidity-shifts for the events from the three different regions of measured asymmetry shown in Fig. 1. Determination of y_0 uses the difference in number of nucleons. For small values of this difference, the changes in values near $y_0 = 0$ are discrete, and are smeared into a continuous distribution as y_0 increases.

generated from a Gaussian distribution of a chosen width σ_y [22]. The pseudorapidity is obtained by using the Blast-Wave model fit to the data for the transverse momentum distributions and the experimentally measured relative yields of pions, kaons and protons [23]. To simulate the effect of different widths of the parent rapidity distribution for different centralities, different σ_y widths are chosen to reproduce the measured FWHM (Full Width at Half Maximum) of the pseudorapidity distribution [24]. For the most central (0–5%) class, a value 3.86 is used for the width of the rapidity distribution, and a value 4.00 is used for the width of the least central class employed in this analysis (30–35%).

The distribution of rapidity-shift y_0, similar to the one shown in Fig. 6, is obtained for each centrality interval and each α_{ZN}^{cut} using TGMC. Fig. 7 (a) shows the $\langle y_0 \rangle$ as a function of α_{ZN}^{cut} for different centralities. One observes a linear relation between the two quantities, showing that an asymmetry in the ZN measurement, arising from the unequal number of participating nucleons, is related to the mean rapidity-shift $\langle y_0 \rangle$. The rapidity distribution of the particles produced in each event is generated assuming a Gaussian form centred about a y_0, which is generated randomly from the y_0 distribution. Events with a rapidity distribution shifted by $y_0 \neq 0$ yield an asymmetric pseudorapidity distribution. A third order polynomial function in η is fitted to the ratio of the simulated $dN/d\eta$ for the asymmetric region to the simulated $dN/d\eta$ for the symmetric region. The values of the coefficients in the expansion depend upon the rapidity-shift y_0 and the parameters characterising the distribution [2].

The simulations described above were repeated for different values of α_{ZN}^{cut} to obtain the pseudorapidity distributions for symmetric and asymmetric regions. Fitting third order polynomial functions to the ratios of the simulated pseudorapidity distributions determines the dependence of c_1 on α_{ZN}^{cut}. Fig. 7 (b) shows that c_1 has a linear dependence on α_{ZN}^{cut} for each centrality interval. The difference in the slopes for different centralities is due to differences in the distributions of y_0 and to differences in the widths of the rapidity distributions.

It is important to note that the parameter c_1, characterising the asymmetry in the pseudorapidity distribution, shows a linear dependence on the parameter α_{ZN}^{cut} in the event sample generated using TGMC and simulations for a Gaussian dN/dy, akin to the dependence of the estimated value of rapidity-shift y_0 for the same sample of events.

5. Results

The longitudinal asymmetry in a heavy-ion collision has been estimated from the difference in the energy of the spectator neutrons on both sides of the collision vertex. The effect of the longitudinal asymmetry is observed in the ratio of $dN/d\eta$ distributions corresponding to different asymmetries. The linear term in a polynomial fit to the distribution of the ratio is dominant, and is characterised by its coefficient c_1. The centrality dependence of the coefficient c_1 for $\alpha_{ZN}^{cut} = 0.1$ is shown in Fig. 8. It is worth emphasising that the values of c_1 and hence its centrality dependence are affected by (i) the distribution of rapidity-shift y_0 for each centrality interval, (ii) the chosen value of α_{ZN}^{cut}, as seen in Fig. 7 and (iii) the shape or the width of the parent rapidity distribution for each centrality. Fig. 8 also shows the results obtained using simulations as described in Sec. 4.2 for $\alpha_{ZN}^{cut} = 0.1$. The systematic uncertainty on the simulated event sample is estimated by (i) varying the resolution of ZNs from 20% to 30%, (ii) assuming all charged particles are pions and (iii) varying the width of the parent rapidity distribution within the range corresponding to the uncertainties on FWHM quoted in Ref. [24]. The simulated events show a good agreement with the experimental data providing cre-

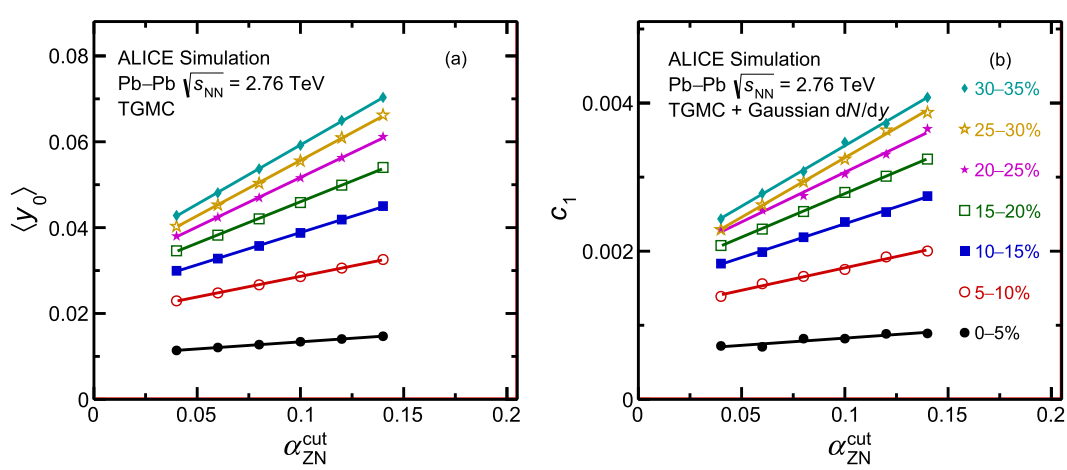

Fig. 7. (a) The estimated mean value of rapidity-shift $\langle y_0 \rangle$ for the asymmetric region characterised by different values of α_{ZN}^{cut} for each centrality interval. (b) The coefficient c_1 characterising the change in the pseudorapidity distributions for different values of α_{ZN}^{cut}, for each centrality interval. These results are obtained using TGMC and simulated pseudorapidity distributions, as described in the text.

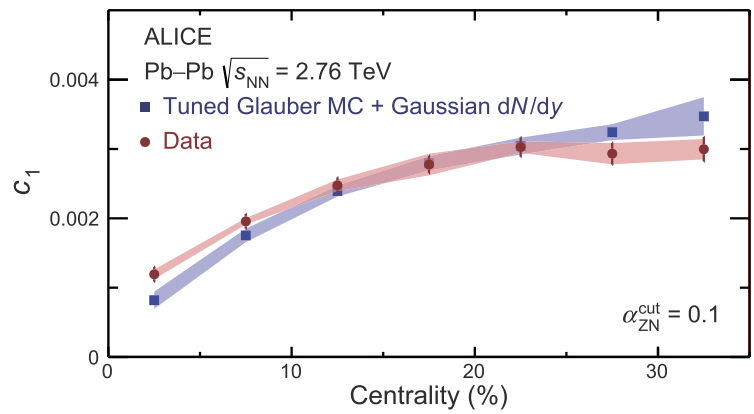

Fig. 8. The mean values of the coefficient c_1 are shown as filled circles for different centralities. These correspond to the ratio of $dN/d\eta$ distributions of populations of events demarcated by $\alpha_{ZN}^{cut} = 0.1$. The squares show the corresponding values from simulations, and correspond to $\alpha_{ZN}^{cut} = 0.1$ in Fig. 7, for different centralities. The systematic uncertainties are shown as bands.

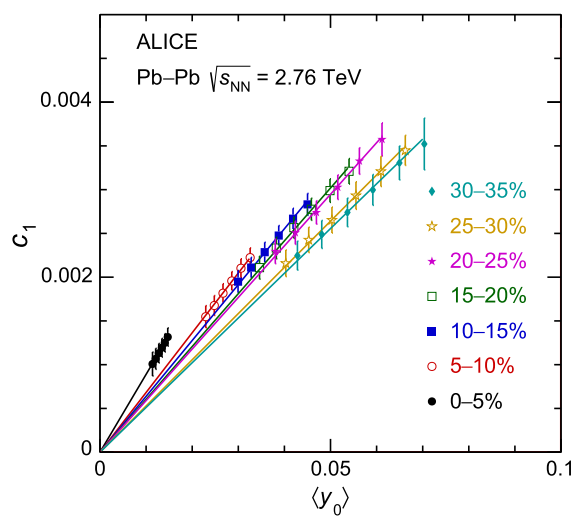

Fig. 9. For each set of events characterised by α_{ZN}^{cut}, the measured values of coefficient c_1 as a function of estimated values of mean rapidity-shift obtained using TGMC as described in the text. The results are shown for different centralities. The uncertainties for $\langle y_0 \rangle$ shown are statistical and within its symbol size. The lines are linear fits passing through the origin.

dence to the assumptions of the simulation, in particular that the asymmetry in the distributions arises from the shift of rapidity of the participant zone.

There are two quantities from independent measurements for each selection of asymmetric events. These are (i) c_1, the parameter characterising the effect of asymmetry in the $dN/d\eta$ distributions and shown in Fig. 3 and (ii) the mean rapidity-shift $\langle y_0 \rangle$ obtained from the measured asymmetry, filtered through the corresponding response matrix (Fig. 4 (d)), and shown in Fig. 7 (a). The relation between c_1 and $\langle y_0 \rangle$ is shown in Fig. 9. The parameter c_1 shows a linear dependence on $\langle y_0 \rangle$ for each centrality. The difference in the slopes indicates the sensitivity of the longitudinal asymmetry to the details of the rapidity distribution. For a Gaussian rapidity distribution the corresponding parameter c_1 would be related to the rapidity-shift as $c_1 = \frac{y_0}{\sigma_{y^2}}$ [2], implying that the slope is inversely proportional to the square of the width of the distribution. The observation of an increase in the slope with an increase in the centrality in the present data indicates a decrease in the width of the pseudorapidity distribution with increasing centrality. Such a decrease in the width of the pseudorapidity distribution with increasing centrality has been observed independently by fitting the pseudorapidity distributions in a broad range of pseudorapidity [24].

6. Conclusions

The present analysis demonstrates the existence of a longitudinal asymmetry in the collision of identical nuclei due to fluctuations in the number of participants from each colliding nucleus. This asymmetry has been measured in the ZNs in the ALICE experiment (Fig. 1), and affects the pseudorapidity distributions, as demonstrated by taking the ratio of distribution of events from the asymmetric region to the corresponding one from the symmetric region (Fig. 2). The effect can be characterised by the coefficient of the linear term in the polynomial expansion of the ratio. The coefficients show a linear dependence on α_{ZN}^{cut}, a parameter to classify the events into symmetric and asymmetric regions (Fig. 3). Different values of α_{ZN}^{cut} correspond to different values of the mean rapidity shift $\langle y_0 \rangle$ (Fig. 7 (a)). The parameter describing the change in the pseudorapidity distributions (c_1) has a simple explanation in the rapidity-shift $\langle y_0 \rangle$ of the participant zone (Fig. 9). The analysis confirms that the longitudinal distributions are affected by the rapidity-shift of the participant zone with respect to the nucleon–nucleon CM frame. The results provide support to the relevance of number of nucleons affecting the production of charged particles, even at such high energies.

The longitudinal asymmetry is a good variable to classify the events and provides information on the initial state of each event. A systematic study of the effects of longitudinal asymmetry on different observables, e.g. the odd harmonics of anisotropic flow, the forward-backward correlations, the source sizes, in heavy-ion collisions may reveal other characteristics of the initial state and of particle production phenomena.

Acknowledgements

The ALICE Collaboration would like to thank all its engineers and technicians for their invaluable contributions to the construction of the experiment and the CERN accelerator teams for the outstanding performance of the LHC complex. The ALICE Collaboration gratefully acknowledges the resources and support provided by all Grid centres and the Worldwide LHC Computing Grid (WLCG) collaboration. The ALICE Collaboration acknowledges the following funding agencies for their support in building and running the ALICE detector: A.I. Alikhanyan National Science Laboratory (Yerevan Physics Institute) Foundation (ANSL), State Committee of Science and World Federation of Scientists (WFS), Armenia;

Austrian Academy of Sciences and Nationalstiftung für Forschung, Technologie und Entwicklung, Austria; Ministry of Communications and High Technologies, National Nuclear Research Center, Azerbaijan; Conselho Nacional de Desenvolvimento Científico e Tecnológico (CNPq), Universidade Federal do Rio Grande do Sul (UFRGS), Financiadora de Estudos e Projetos (Finep) and Fundação de Amparo à Pesquisa do Estado de São Paulo (FAPESP), Brazil; Ministry of Science & Technology of China (MSTC), National Natural Science Foundation of China (NSFC) and Ministry of Education of China (MOEC), China; Ministry of Science, Education and Sport and Croatian Science Foundation, Croatia; Ministry of Education, Youth and Sports of the Czech Republic, Czech Republic; The Danish Council for Independent Research | Natural Sciences, the Carlsberg Foundation and Danish National Research Foundation (DNRF), Denmark; Helsinki Institute of Physics (HIP), Finland; Commissariat à l'Energie Atomique (CEA) and Institut National de Physique Nucléaire et de Physique des Particules (IN2P3) and Centre National de la Recherche Scientifique (CNRS), France; Bundesministerium für Bildung, Wissenschaft, Forschung und Technologie (BMBF) and GSI Helmholtzzentrum für Schwerionenforschung GmbH, Germany; General Secretariat for Research and Technology, Ministry of Education, Research and Religions, Greece; National Research, Development and Innovation Office, Hungary; Department of Atomic Energy, Government of India (DAE), Department of Science and Technology, Government of India (DST), University Grants Commission, Government of India (UGC) and Council of Scientific and Industrial Research (CSIR), India; Indonesian Institute of Science, Indonesia; Centro Fermi – Museo Storico della Fisica e Centro Studi e Ricerche Enrico Fermi and Istituto Nazionale di Fisica Nucleare (INFN), Italy; Institute for Innovative Science and Technology, Nagasaki Institute of Applied Science (IIST), Japan Society for the Promotion of Science (JSPS) KAKENHI and Japanese Ministry of Education, Culture, Sports, Science and Technology (MEXT), Japan; Consejo Nacional de Ciencia (CONACYT) y Tecnología, through Fondo de Cooperación Internacional en Ciencia y Tecnología (FONCICYT) and Dirección General de Asuntos del Personal Academico (DGAPA), Mexico; Nederlandse Organisatie voor Wetenschappelijk Onderzoek (NWO), Netherlands; The Research Council of Norway, Norway; Commission on Science and Technology for Sustainable Development in the South (COMSATS), Pakistan; Pontificia Universidad Católica del Perú, Peru; Ministry of Science and Higher Education and National Science Centre, Poland; Korea Institute of Science and Technology Information and National Research Foundation of Korea (NRF), Republic of Korea; Ministry of Education and Scientific Research, Institute of Atomic Physics and Romanian National Agency for Science, Technology and Innovation, Romania; Joint Institute for Nuclear Research (JINR), Ministry of Education and Science of the Russian Federation and National Research Centre Kurchatov Institute, Russia; Ministry of Education, Science, Research and Sport of the Slovak Republic, Slovakia; National Research Foundation of South Africa, South Africa; Centro de Aplicaciones Tecnológicas y Desarrollo Nuclear (CEADEN), Cubaenergía, Cuba, Ministerio de Ciencia e Innovacion and Centro de Investigaciones Energéticas, Medioambientales y Tecnológicas (CIEMAT), Spain; Swedish Research Council (VR) and Knut & Alice Wallenberg Foundation (KAW), Sweden; European Organization for Nuclear Research, Switzerland; National Science and Technology Development Agency (NSDTA), Suranaree University of Technology (SUT) and Office of the Higher Education Commission under NRU project of Thailand, Thailand; Turkish Atomic Energy Agency (TAEK), Turkey; National Academy of Sciences of Ukraine, Ukraine; Science and Technology Facilities Council (STFC), United Kingdom; National Science Foundation of the United States of America (NSF) and United States Department of Energy, Office of Nuclear Physics (DOE NP), United States of America.

References

[1] V. Vovchenko, D. Anchishkin, L.P. Csernai, Longitudinal fluctuations of the center of mass of the participants in heavy-ion collisions, Phys. Rev. C 88 (1) (2013) 014901, arXiv:1306.5208 [nucl-th].

[2] R. Raniwala, S. Raniwala, C. Loizides, Effects of longitudinal asymmetry in heavy-ion collisions, Phys. Rev. C 97 (2) (2018) 024912, arXiv:1608.01428 [nucl-ex].

[3] STAR Collaboration, L. Adamczyk, et al., Global Λ hyperon polarization in nuclear collisions: evidence for the most vortical fluid, Nature 548 (2017) 62–65, arXiv:1701.06657 [nucl-ex].

[4] F. Becattini, L. Csernai, D.J. Wang, Λ polarization in peripheral heavy ion collisions, Phys. Rev. C 88 (3) (2013) 034905, arXiv:1304.4427 [nucl-th]; Erratum Phys. Rev. C 93 (6) (2016) 069901.

[5] Y. Xie, D. Wang, L.P. Csernai, Global Λ polarization in high energy collisions, Phys. Rev. C 95 (3) (2017) 031901, arXiv:1703.03770 [nucl-th].

[6] ALICE Collaboration, J. Adam, et al., Event shape engineering for inclusive spectra and elliptic flow in Pb–Pb collisions at $\sqrt{s_{\rm NN}} = 2.76$ TeV, Phys. Rev. C 93 (3) (2016) 034916, arXiv:1507.06194 [nucl-ex].

[7] PHOBOS Collaboration, B.B. Back, et al., Pseudorapidity distribution of charged particles in d + Au collisions at $s(\mathrm{NN})^{**}(1/2) = 200$-GeV, Phys. Rev. Lett. 93 (2004) 082301, arXiv:nucl-ex/0311009.

[8] ALICE Collaboration, B. Abelev, et al., Pseudorapidity density of charged particles in p + Pb collisions at $\sqrt{s_{NN}} = 5.02$ TeV, Phys. Rev. Lett. 110 (3) (2013) 032301, arXiv:1210.3615 [nucl-ex].

[9] ALICE Collaboration, J. Adam, et al., Centrality dependence of particle production in p-Pb collisions at $\sqrt{s_{\rm NN}} = 5.02$ TeV, Phys. Rev. C 91 (6) (2015) 064905, arXiv:1412.6828 [nucl-ex].

[10] ATLAS Collaboration, G. Aad, et al., Measurement of the centrality dependence of the charged-particle pseudorapidity distribution in proton–lead collisions at $\sqrt{s_{\rm NN}} = 5.02$ TeV with the ATLAS detector, Eur. Phys. J. C 76 (4) (2016) 199, arXiv:1508.00848 [hep-ex].

[11] P. Steinberg, Inclusive pseudorapidity distributions in p(d) + A collisions modeled with shifted rapidity distributions, Phys. Lett. B (2007), submitted for publication, arXiv:nucl-ex/0703002.

[12] A. Bzdak, D. Teaney, Longitudinal fluctuations of the fireball density in heavy-ion collisions, Phys. Rev. C 87 (2) (2013) 024906, arXiv:1210.1965 [nucl-th].

[13] J. Jia, S. Radhakrishnan, M. Zhou, Forward–backward multiplicity fluctuation and longitudinal harmonics in high-energy nuclear collisions, Phys. Rev. C 93 (4) (2016) 044905, arXiv:1506.03496 [nucl-th].

[14] ATLAS Collaboration, M. Aaboud, et al., Measurement of forward–backward multiplicity correlations in lead–lead, proton–lead, and proton–proton collisions with the ATLAS detector, Phys. Rev. C 95 (6) (2017) 064914, arXiv:1606.08170 [hep-ex].

[15] ALICE Collaboration, K. Aamodt, et al., Elliptic flow of charged particles in Pb–Pb collisions at 2.76 TeV, Phys. Rev. Lett. 105 (2010) 252302, arXiv:1011.3914 [nucl-ex].

[16] ALICE Collaboration, K. Aamodt, et al., Centrality dependence of the charged-particle multiplicity density at mid-rapidity in Pb–Pb collisions at $\sqrt{s_{\rm NN}} = 2.76$ TeV, Phys. Rev. Lett. 106 (2011) 032301, arXiv:1012.1657 [nucl-ex].

[17] ALICE Collaboration, K. Aamodt, et al., The ALICE experiment at the CERN LHC, J. Instrum. 3 (2008) S08002.

[18] ALICE Collaboration, B.B. Abelev, et al., Performance of the ALICE experiment at the CERN LHC, Int. J. Mod. Phys. A 29 (2014) 1430044, arXiv:1402.4476 [nucl-ex].

[19] ALICE Collaboration, B. Abelev, et al., Measurement of the cross section for electromagnetic dissociation with neutron emission in Pb–Pb collisions at $\sqrt{s_{\rm NN}} = 2.76$ TeV, Phys. Rev. Lett. 109 (2012) 252302, arXiv:1203.2436 [nucl-ex].

[20] ALICE Collaboration, B. Abelev, et al., Centrality determination of Pb–Pb collisions at $\sqrt{s_{\rm NN}} = 2.76$ TeV with ALICE, Phys. Rev. C 88 (4) (2013) 044909, arXiv:1301.4361 [nucl-ex].

[21] B. Alver, M. Baker, C. Loizides, P. Steinberg, The PHOBOS Glauber Monte Carlo, arXiv:0805.4411 [nucl-ex].

[22] ALICE Collaboration, E. Abbas, et al., Centrality dependence of the pseudorapidity density distribution for charged particles in Pb–Pb collisions at $\sqrt{s_{\rm NN}} = 2.76$ TeV, Phys. Lett. B 726 (2013) 610–622, arXiv:1304.0347 [nucl-ex].

[23] ALICE Collaboration, B. Abelev, et al., Centrality dependence of π, K, p production in Pb–Pb collisions at $\sqrt{s_{\rm NN}} = 2.76$ TeV, Phys. Rev. C 88 (2013) 044910, arXiv:1303.0737 [hep-ex].

[24] ALICE Collaboration, J. Adam, et al., Centrality evolution of the charged-particle pseudorapidity density over a broad pseudorapidity range in Pb–Pb collisions at $\sqrt{s_{\rm NN}} = 2.76$ TeV, Phys. Lett. B 754 (2016) 373–385, arXiv:1509.07299 [nucl-ex].

ALICE Collaboration

S. Acharya [137], J. Adam [96], D. Adamová [93], J. Adolfsson [32], M.M. Aggarwal [98], G. Aglieri Rinella [33], M. Agnello [29], N. Agrawal [46], Z. Ahammed [137], N. Ahmad [15], S.U. Ahn [78], S. Aiola [141], A. Akindinov [63], M. Al-Turany [106], S.N. Alam [137], J.L.B. Alba [111], D.S.D. Albuquerque [122], D. Aleksandrov [89], B. Alessandro [57], R. Alfaro Molina [73], A. Alici [11,25,52], A. Alkin [3], J. Alme [20], T. Alt [69], L. Altenkamper [20], I. Altsybeev [136], C. Alves Garcia Prado [121], C. Andrei [86], D. Andreou [33], H.A. Andrews [110], A. Andronic [106], V. Anguelov [103], C. Anson [96], T. Antičić [107], F. Antinori [55], P. Antonioli [52], R. Anwar [124], L. Aphecetche [114], H. Appelshäuser [69], S. Arcelli [25], R. Arnaldi [57], O.W. Arnold [104,34], I.C. Arsene [19], M. Arslandok [103], B. Audurier [114], A. Augustinus [33], R. Averbeck [106], M.D. Azmi [15], A. Badalà [54], Y.W. Baek [59,77], S. Bagnasco [57], R. Bailhache [69], R. Bala [100], A. Baldisseri [74], M. Ball [43], R.C. Baral [66,87], A.M. Barbano [24], R. Barbera [26], F. Barile [51,31], L. Barioglio [24], G.G. Barnaföldi [140], L.S. Barnby [92], V. Barret [131], P. Bartalini [7], K. Barth [33], E. Bartsch [69], M. Basile [25], N. Bastid [131], S. Basu [139], G. Batigne [114], B. Batyunya [76], P.C. Batzing [19], I.G. Bearden [90], H. Beck [103], C. Bedda [62], N.K. Behera [59], I. Belikov [133], F. Bellini [25,33], H. Bello Martinez [2], R. Bellwied [124], L.G.E. Beltran [120], V. Belyaev [82], G. Bencedi [140], S. Beole [24], A. Bercuci [86], Y. Berdnikov [95], D. Berenyi [140], R.A. Bertens [127], D. Berzano [33], L. Betev [33], A. Bhasin [100], I.R. Bhat [100], A.K. Bhati [98], B. Bhattacharjee [42], J. Bhom [118], A. Bianchi [24], L. Bianchi [124], N. Bianchi [49], C. Bianchin [139], J. Bielčík [37], J. Bielčíková [93], A. Bilandzic [34,104], G. Biro [140], R. Biswas [4], S. Biswas [4], J.T. Blair [119], D. Blau [89], C. Blume [69], G. Boca [134], F. Bock [81,33,103], A. Bogdanov [82], L. Boldizsár [140], M. Bombara [38], G. Bonomi [135], M. Bonora [33], J. Book [69], H. Borel [74], A. Borissov [103,17], M. Borri [126], E. Botta [24], C. Bourjau [90], L. Bratrud [69], P. Braun-Munzinger [106], M. Bregant [121], T.A. Broker [69], M. Broz [37], E.J. Brucken [44], E. Bruna [57], G.E. Bruno [33,31], D. Budnikov [108], H. Buesching [69], S. Bufalino [29], P. Buhler [113], P. Buncic [33], O. Busch [130], Z. Buthelezi [75], J.B. Butt [14], J.T. Buxton [16], J. Cabala [116], D. Caffarri [33,91], H. Caines [141], A. Caliva [62,106], E. Calvo Villar [111], P. Camerini [23], A.A. Capon [113], F. Carena [33], W. Carena [33], F. Carnesecchi [25,11], J. Castillo Castellanos [74], A.J. Castro [127], E.A.R. Casula [53], C. Ceballos Sanchez [9], P. Cerello [57], S. Chandra [137], B. Chang [125], S. Chapeland [33], M. Chartier [126], S. Chattopadhyay [137], S. Chattopadhyay [109], A. Chauvin [34,104], C. Cheshkov [132], B. Cheynis [132], V. Chibante Barroso [33], D.D. Chinellato [122], S. Cho [59], P. Chochula [33], M. Chojnacki [90], S. Choudhury [137], T. Chowdhury [131], P. Christakoglou [91], C.H. Christensen [90], P. Christiansen [32], T. Chujo [130], S.U. Chung [17], C. Cicalo [53], L. Cifarelli [11,25], F. Cindolo [52], J. Cleymans [99], F. Colamaria [31], D. Colella [33,64,51], A. Collu [81], M. Colocci [25], M. Concas [57,ii], G. Conesa Balbastre [80], Z. Conesa del Valle [60], M.E. Connors [141,iii], J.G. Contreras [37], T.M. Cormier [94], Y. Corrales Morales [57], I. Cortés Maldonado [2], P. Cortese [30], M.R. Cosentino [123], F. Costa [33], S. Costanza [134], J. Crkovská [60], P. Crochet [131], E. Cuautle [71], L. Cunqueiro [70], T. Dahms [34,104], A. Dainese [55], M.C. Danisch [103], A. Danu [67], D. Das [109], I. Das [109], S. Das [4], A. Dash [87], S. Dash [46], S. De [47,121], A. De Caro [28], G. de Cataldo [51], C. de Conti [121], J. de Cuveland [40], A. De Falco [22], D. De Gruttola [28,11], N. De Marco [57], S. De Pasquale [28], R.D. De Souza [122], H.F. Degenhardt [121], A. Deisting [106,103], A. Deloff [85], C. Deplano [91], P. Dhankher [46], D. Di Bari [31], A. Di Mauro [33], P. Di Nezza [49], B. Di Ruzza [55], T. Dietel [99], P. Dillenseger [69], R. Divià [33], Ø. Djuvsland [20], A. Dobrin [33], D. Domenicis Gimenez [121], B. Dönigus [69], O. Dordic [19], L.V.R. Doremalen [62], A.K. Dubey [137], A. Dubla [106], L. Ducroux [132], A.K. Duggal [98], M. Dukhishyam [87], P. Dupieux [131], R.J. Ehlers [141], D. Elia [51], E. Endress [111], H. Engel [68], E. Epple [141], B. Erazmus [114], F. Erhardt [97], B. Espagnon [60], S. Esumi [130], G. Eulisse [33], J. Eum [17], D. Evans [110], S. Evdokimov [112], L. Fabbietti [104,34], J. Faivre [80], A. Fantoni [49], M. Fasel [94,81], L. Feldkamp [70], A. Feliciello [57], G. Feofilov [136], A. Fernández Téllez [2], A. Ferretti [24], A. Festanti [27,33], V.J.G. Feuillard [74,131], J. Figiel [118], M.A.S. Figueredo [121], S. Filchagin [108], D. Finogeev [61], F.M. Fionda [20,22], M. Floris [33], S. Foertsch [75], P. Foka [106], S. Fokin [89], E. Fragiacomo [58], A. Francescon [33], A. Francisco [114], U. Frankenfeld [106], G.G. Fronze [24], U. Fuchs [33], C. Furget [80], A. Furs [61], M. Fusco Girard [28], J.J. Gaardhøje [90], M. Gagliardi [24], A.M. Gago [111], K. Gajdosova [90], M. Gallio [24], C.D. Galvan [120], P. Ganoti [84], C. Garabatos [106], E. Garcia-Solis [12], K. Garg [26], C. Gargiulo [33], P. Gasik [104,34], E.F. Gauger [119], M.B. Gay Ducati [72], M. Germain [114], J. Ghosh [109], P. Ghosh [137], S.K. Ghosh [4], P. Gianotti [49], P. Giubellino [106,33,57], P. Giubilato [27], E. Gladysz-Dziadus [118], P. Glässel [103], D.M. Goméz Coral [73], A. Gomez Ramirez [68], A.S. Gonzalez [33], P. González-Zamora [2], S. Gorbunov [40], L. Görlich [118], S. Gotovac [117], V. Grabski [73], L.K. Graczykowski [138], K.L. Graham [110], L. Greiner [81], A. Grelli [62], C. Grigoras [33], V. Grigoriev [82], A. Grigoryan [1], S. Grigoryan [76], J.M. Gronefeld [106], F. Grosa [29], J.F. Grosse-Oetringhaus [33], R. Grosso [106], L. Gruber [113], F. Guber [61],

R. Guernane [80], B. Guerzoni [25], K. Gulbrandsen [90], T. Gunji [129], A. Gupta [100], R. Gupta [100], I.B. Guzman [2], R. Haake [33], C. Hadjidakis [60], H. Hamagaki [83], G. Hamar [140], J.C. Hamon [133], M.R. Haque [62], J.W. Harris [141], A. Harton [12], H. Hassan [80], D. Hatzifotiadou [11,52], S. Hayashi [129], S.T. Heckel [69], E. Hellbär [69], H. Helstrup [35], A. Herghelegiu [86], E.G. Hernandez [2], G. Herrera Corral [10], F. Herrmann [70], B.A. Hess [102], K.F. Hetland [35], H. Hillemanns [33], C. Hills [126], B. Hippolyte [133], J. Hladky [65], B. Hohlweger [104], D. Horak [37], S. Hornung [106], R. Hosokawa [80,130], P. Hristov [33], C. Hughes [127], T.J. Humanic [16], N. Hussain [42], T. Hussain [15], D. Hutter [40], D.S. Hwang [18], S.A. Iga Buitron [71], R. Ilkaev [108], M. Inaba [130], M. Ippolitov [82,89], M. Irfan [15], M.S. Islam [109], M. Ivanov [106], V. Ivanov [95], V. Izucheev [112], B. Jacak [81], N. Jacazio [25], P.M. Jacobs [81], M.B. Jadhav [46], J. Jadlovsky [116], S. Jaelani [62], C. Jahnke [34], M.J. Jakubowska [138], M.A. Janik [138], P.H.S.Y. Jayarathna [124], C. Jena [87], S. Jena [124], M. Jercic [97], R.T. Jimenez Bustamante [106], P.G. Jones [110], A. Jusko [110], P. Kalinak [64], A. Kalweit [33], J.H. Kang [142], V. Kaplin [82], S. Kar [137], A. Karasu Uysal [79], O. Karavichev [61], T. Karavicheva [61], L. Karayan [106,103], P. Karczmarczyk [33], E. Karpechev [61], U. Kebschull [68], R. Keidel [143], D.L.D. Keijdener [62], M. Keil [33], B. Ketzer [43], Z. Khabanova [91], P. Khan [109], S.A. Khan [137], A. Khanzadeev [95], Y. Kharlov [112], A. Khatun [15], A. Khuntia [47], M.M. Kielbowicz [118], B. Kileng [35], B. Kim [130], D. Kim [142], D.J. Kim [125], H. Kim [142], J.S. Kim [41], J. Kim [103], M. Kim [59], M. Kim [142], S. Kim [18], T. Kim [142], S. Kirsch [40], I. Kisel [40], S. Kiselev [63], A. Kisiel [138], G. Kiss [140], J.L. Klay [6], C. Klein [69], J. Klein [33], C. Klein-Bösing [70], S. Klewin [103], A. Kluge [33], M.L. Knichel [103,33], A.G. Knospe [124], C. Kobdaj [115], M. Kofarago [140], M.K. Köhler [103], T. Kollegger [106], V. Kondratiev [136], N. Kondratyeva [82], E. Kondratyuk [112], A. Konevskikh [61], M. Konyushikhin [139], M. Kopcik [116], M. Kour [100], C. Kouzinopoulos [33], O. Kovalenko [85], V. Kovalenko [136], M. Kowalski [118], G. Koyithatta Meethaleveedu [46], I. Králik [64], A. Kravčáková [38], L. Kreis [106], M. Krivda [110,64], F. Krizek [93], E. Kryshen [95], M. Krzewicki [40], A.M. Kubera [16], V. Kučera [93], C. Kuhn [133], P.G. Kuijer [91], A. Kumar [100], J. Kumar [46], L. Kumar [98], S. Kumar [46], S. Kundu [87], P. Kurashvili [85], A. Kurepin [61], A.B. Kurepin [61], A. Kuryakin [108], S. Kushpil [93], M.J. Kweon [59], Y. Kwon [142], S.L. La Pointe [40], P. La Rocca [26], C. Lagana Fernandes [121], Y.S. Lai [81], I. Lakomov [33], R. Langoy [39], K. Lapidus [141], C. Lara [68], A. Lardeux [74,19], A. Lattuca [24], E. Laudi [33], R. Lavicka [37], R. Lea [23], L. Leardini [103], S. Lee [142], F. Lehas [91], S. Lehner [113], J. Lehrbach [40], R.C. Lemmon [92], V. Lenti [51], E. Leogrande [62], I. León Monzón [120], P. Lévai [140], X. Li [13], J. Lien [39], R. Lietava [110], B. Lim [17], S. Lindal [19], V. Lindenstruth [40], S.W. Lindsay [126], C. Lippmann [106], M.A. Lisa [16], V. Litichevskyi [44], W.J. Llope [139], D.F. Lodato [62], P.I. Loenne [20], V. Loginov [82], C. Loizides [81], P. Loncar [117], X. Lopez [131], E. López Torres [9], A. Lowe [140], P. Luettig [69], J.R. Luhder [70], M. Lunardon [27], G. Luparello [58,23], M. Lupi [33], T.H. Lutz [141], A. Maevskaya [61], M. Mager [33], S. Mahajan [100], S.M. Mahmood [19], A. Maire [133], R.D. Majka [141], M. Malaev [95], L. Malinina [76,iv], D. Mal'Kevich [63], P. Malzacher [106], A. Mamonov [108], V. Manko [89], F. Manso [131], V. Manzari [51], Y. Mao [7], M. Marchisone [75,128], J. Mareš [65], G.V. Margagliotti [23], A. Margotti [52], J. Margutti [62], A. Marín [106], C. Markert [119], M. Marquard [69], N.A. Martin [106], P. Martinengo [33], J.A.L. Martinez [68], M.I. Martínez [2], G. Martínez García [114], M. Martinez Pedreira [33], S. Masciocchi [106], M. Masera [24], A. Masoni [53], E. Masson [114], A. Mastroserio [51], A.M. Mathis [104,34], P.F.T. Matuoka [121], A. Matyja [127], C. Mayer [118], J. Mazer [127], M. Mazzilli [31], M.A. Mazzoni [56], F. Meddi [21], Y. Melikyan [82], A. Menchaca-Rocha [73], E. Meninno [28], J. Mercado Pérez [103], M. Meres [36], S. Mhlanga [99], Y. Miake [130], M.M. Mieskolainen [44], D.L. Mihaylov [104], K. Mikhaylov [63,76], J. Milosevic [19], A. Mischke [62], A.N. Mishra [47], D. Miśkowiec [106], J. Mitra [137], C.M. Mitu [67], N. Mohammadi [62], B. Mohanty [87], M. Mohisin Khan [15,v], D.A. Moreira De Godoy [70], L.A.P. Moreno [2], S. Moretto [27], A. Morreale [114], A. Morsch [33], V. Muccifora [49], E. Mudnic [117], D. Mühlheim [70], S. Muhuri [137], M. Mukherjee [4], J.D. Mulligan [141], M.G. Munhoz [121], K. Münning [43], R.H. Munzer [69], H. Murakami [129], S. Murray [75], L. Musa [33], J. Musinsky [64], C.J. Myers [124], J.W. Myrcha [138], D. Nag [4], B. Naik [46], R. Nair [85], B.K. Nandi [46], R. Nania [52,11], E. Nappi [51], A. Narayan [46], M.U. Naru [14], H. Natal da Luz [121], C. Nattrass [127], S.R. Navarro [2], K. Nayak [87], R. Nayak [46], T.K. Nayak [137], S. Nazarenko [108], A. Nedosekin [63], R.A. Negrao De Oliveira [33], L. Nellen [71], S.V. Nesbo [35], F. Ng [124], M. Nicassio [106], M. Niculescu [67], J. Niedziela [138,33], B.S. Nielsen [90], S. Nikolaev [89], S. Nikulin [89], V. Nikulin [95], F. Noferini [11,52], P. Nomokonov [76], G. Nooren [62], J.C.C. Noris [2], J. Norman [126], A. Nyanin [89], J. Nystrand [20], H. Oeschler [17,103,i], S. Oh [141], A. Ohlson [33,103], T. Okubo [45], L. Olah [140], J. Oleniacz [138], A.C. Oliveira Da Silva [121], M.H. Oliver [141], J. Onderwaater [106], C. Oppedisano [57], R. Orava [44], M. Oravec [116], A. Ortiz Velasquez [71], A. Oskarsson [32], J. Otwinowski [118], K. Oyama [83], Y. Pachmayer [103], V. Pacik [90], D. Pagano [135], P. Pagano [28], G. Paić [71], P. Palni [7], J. Pan [139], A.K. Pandey [46], S. Panebianco [74], V. Papikyan [1],

G.S. Pappalardo [54], P. Pareek [47], J. Park [59], S. Parmar [98], A. Passfeld [70], S.P. Pathak [124], R.N. Patra [137], B. Paul [57], H. Pei [7], T. Peitzmann [62], X. Peng [7], L.G. Pereira [72], H. Pereira Da Costa [74], D. Peresunko [89,82], E. Perez Lezama [69], V. Peskov [69], Y. Pestov [5], V. Petráček [37], V. Petrov [112], M. Petrovici [86], C. Petta [26], R.P. Pezzi [72], S. Piano [58], M. Pikna [36], P. Pillot [114], L.O.D.L. Pimentel [90], O. Pinazza [52,33], L. Pinsky [124], D.B. Piyarathna [124], M. Płoskoń [81], M. Planinic [97], F. Pliquett [69], J. Pluta [138], S. Pochybova [140], P.L.M. Podesta-Lerma [120], M.G. Poghosyan [94], B. Polichtchouk [112], N. Poljak [97], W. Poonsawat [115], A. Pop [86], H. Poppenborg [70], S. Porteboeuf-Houssais [131], V. Pozdniakov [76], S.K. Prasad [4], R. Preghenella [52], F. Prino [57], C.A. Pruneau [139], I. Pshenichnov [61], M. Puccio [24], G. Puddu [22], P. Pujahari [139], V. Punin [108], J. Putschke [139], S. Raha [4], S. Rajput [100], J. Rak [125], A. Rakotozafindrabe [74], L. Ramello [30], F. Rami [133], D.B. Rana [124], R. Raniwala [101], S. Raniwala [101], S.S. Räsänen [44], B.T. Rascanu [69], D. Rathee [98], V. Ratza [43], I. Ravasenga [29], K.F. Read [127,94], K. Redlich [85,vi], A. Rehman [20], P. Reichelt [69], F. Reidt [33], X. Ren [7], R. Renfordt [69], A.R. Reolon [49], A. Reshetin [61], K. Reygers [103], V. Riabov [95], R.A. Ricci [50], T. Richert [32], M. Richter [19], P. Riedler [33], W. Riegler [33], F. Riggi [26], C. Ristea [67], M. Rodríguez Cahuantzi [2], K. Røed [19], E. Rogochaya [76], D. Rohr [33,40], D. Röhrich [20], P.S. Rokita [138], F. Ronchetti [49], E.D. Rosas [71], P. Rosnet [131], A. Rossi [27,55], A. Rotondi [134], F. Roukoutakis [84], A. Roy [47], C. Roy [133], P. Roy [109], O.V. Rueda [71], R. Rui [23], B. Rumyantsev [76], A. Rustamov [88], E. Ryabinkin [89], Y. Ryabov [95], A. Rybicki [118], S. Saarinen [44], S. Sadhu [137], S. Sadovsky [112], K. Šafařík [33], S.K. Saha [137], B. Sahlmuller [69], B. Sahoo [46], P. Sahoo [47], R. Sahoo [47], S. Sahoo [66], P.K. Sahu [66], J. Saini [137], S. Sakai [130], M.A. Saleh [139], J. Salzwedel [16], S. Sambyal [100], V. Samsonov [95,82], A. Sandoval [73], D. Sarkar [137], N. Sarkar [137], P. Sarma [42], M.H.P. Sas [62], E. Scapparone [52], F. Scarlassara [27], B. Schaefer [94], R.P. Scharenberg [105], H.S. Scheid [69], C. Schiaua [86], R. Schicker [103], C. Schmidt [106], H.R. Schmidt [102], M.O. Schmidt [103], M. Schmidt [102], N.V. Schmidt [94,69], J. Schukraft [33], Y. Schutz [33,133], K. Schwarz [106], K. Schweda [106], G. Scioli [25], E. Scomparin [57], M. Šefčík [38], J.E. Seger [96], Y. Sekiguchi [129], D. Sekihata [45], I. Selyuzhenkov [106,82], K. Senosi [75], S. Senyukov [3,133,33], E. Serradilla [73], P. Sett [46], A. Sevcenco [67], A. Shabanov [61], A. Shabetai [114], R. Shahoyan [33], W. Shaikh [109], A. Shangaraev [112], A. Sharma [98], A. Sharma [100], M. Sharma [100], M. Sharma [100], N. Sharma [98,127], A.I. Sheikh [137], K. Shigaki [45], Q. Shou [7], K. Shtejer [9,24], Y. Sibiriak [89], S. Siddhanta [53], K.M. Sielewicz [33], T. Siemiarczuk [85], S. Silaeva [89], D. Silvermyr [32], C. Silvestre [80], G. Simatovic [97], G. Simonetti [33], R. Singaraju [137], R. Singh [87], V. Singhal [137], T. Sinha [109], B. Sitar [36], M. Sitta [30], T.B. Skaali [19], M. Slupecki [125], N. Smirnov [141], R.J.M. Snellings [62], T.W. Snellman [125], J. Song [17], M. Song [142], F. Soramel [27], S. Sorensen [127], F. Sozzi [106], E. Spiriti [49], I. Sputowska [118], B.K. Srivastava [105], J. Stachel [103], I. Stan [67], P. Stankus [94], E. Stenlund [32], D. Stocco [114], M.M. Storetvedt [35], P. Strmen [36], A.A.P. Suaide [121], T. Sugitate [45], C. Suire [60], M. Suleymanov [14], M. Suljic [23], R. Sultanov [63], M. Šumbera [93], S. Sumowidagdo [48], K. Suzuki [113], S. Swain [66], A. Szabo [36], I. Szarka [36], U. Tabassam [14], J. Takahashi [122], G.J. Tambave [20], N. Tanaka [130], M. Tarhini [60], M. Tariq [15], M.G. Tarzila [86], A. Tauro [33], G. Tejeda Muñoz [2], A. Telesca [33], K. Terasaki [129], C. Terrevoli [27], B. Teyssier [132], D. Thakur [47], S. Thakur [137], D. Thomas [119], F. Thoresen [90], R. Tieulent [132], A. Tikhonov [61], A.R. Timmins [124], A. Toia [69], S.R. Torres [120], S. Tripathy [47], S. Trogolo [24], G. Trombetta [31], L. Tropp [38], V. Trubnikov [3], W.H. Trzaska [125], B.A. Trzeciak [62], T. Tsuji [129], A. Tumkin [108], R. Turrisi [55], T.S. Tveter [19], K. Ullaland [20], E.N. Umaka [124], A. Uras [132], G.L. Usai [22], A. Utrobicic [97], M. Vala [116,64], J. Van Der Maarel [62], J.W. Van Hoorne [33], M. van Leeuwen [62], T. Vanat [93], P. Vande Vyvre [33], D. Varga [140], A. Vargas [2], M. Vargyas [125], R. Varma [46], M. Vasileiou [84], A. Vasiliev [89], A. Vauthier [80], O. Vázquez Doce [104,34], V. Vechernin [136], A.M. Veen [62], A. Velure [20], E. Vercellin [24], S. Vergara Limón [2], R. Vernet [8], R. Vértesi [140], L. Vickovic [117], S. Vigolo [62], J. Viinikainen [125], Z. Vilakazi [128], O. Villalobos Baillie [110], A. Villatoro Tello [2], A. Vinogradov [89], L. Vinogradov [136], T. Virgili [28], V. Vislavicius [32], A. Vodopyanov [76], M.A. Völkl [103,102], K. Voloshin [63], S.A. Voloshin [139], G. Volpe [31], B. von Haller [33], I. Vorobyev [104,34], D. Voscek [116], D. Vranic [33,106], J. Vrláková [38], B. Wagner [20], H. Wang [62], M. Wang [7], D. Watanabe [130], Y. Watanabe [129,130], M. Weber [113], S.G. Weber [106], D.F. Weiser [103], S.C. Wenzel [33], J.P. Wessels [70], U. Westerhoff [70], A.M. Whitehead [99], J. Wiechula [69], J. Wikne [19], G. Wilk [85], J. Wilkinson [103,52], G.A. Willems [33,70], M.C.S. Williams [52], E. Willsher [110], B. Windelband [103], W.E. Witt [127], S. Yalcin [79], K. Yamakawa [45], P. Yang [7], S. Yano [45], Z. Yin [7], H. Yokoyama [130,80], I.-K. Yoo [17], J.H. Yoon [59], V. Yurchenko [3], V. Zaccolo [57], A. Zaman [14], C. Zampolli [33], H.J.C. Zanoli [121], N. Zardoshti [110], A. Zarochentsev [136], P. Závada [65], N. Zaviyalov [108], H. Zbroszczyk [138], M. Zhalov [95], H. Zhang [20,7], X. Zhang [7], Y. Zhang [7], C. Zhang [62],

Z. Zhang [7,131], C. Zhao [19], N. Zhigareva [63], D. Zhou [7], Y. Zhou [90], Z. Zhou [20], H. Zhu [20], J. Zhu [7], A. Zichichi [25,11], A. Zimmermann [103], M.B. Zimmermann [33], G. Zinovjev [3], J. Zmeskal [113], S. Zou [7]

[1] A.I. Alikhanyan National Science Laboratory (Yerevan Physics Institute) Foundation, Yerevan, Armenia
[2] Benemérita Universidad Autónoma de Puebla, Puebla, Mexico
[3] Bogolyubov Institute for Theoretical Physics, Kiev, Ukraine
[4] Bose Institute, Department of Physics and Centre for Astroparticle Physics and Space Science (CAPSS), Kolkata, India
[5] Budker Institute for Nuclear Physics, Novosibirsk, Russia
[6] California Polytechnic State University, San Luis Obispo, CA, United States
[7] Central China Normal University, Wuhan, China
[8] Centre de Calcul de l'IN2P3, Villeurbanne, Lyon, France
[9] Centro de Aplicaciones Tecnológicas y Desarrollo Nuclear (CEADEN), Havana, Cuba
[10] Centro de Investigación y de Estudios Avanzados (CINVESTAV), Mexico City and Mérida, Mexico
[11] Centro Fermi – Museo Storico della Fisica e Centro Studi e Ricerche "Enrico Fermi', Rome, Italy
[12] Chicago State University, Chicago, IL, United States
[13] China Institute of Atomic Energy, Beijing, China
[14] COMSATS Institute of Information Technology (CIIT), Islamabad, Pakistan
[15] Department of Physics, Aligarh Muslim University, Aligarh, India
[16] Department of Physics, Ohio State University, Columbus, OH, United States
[17] Department of Physics, Pusan National University, Pusan, Republic of Korea
[18] Department of Physics, Sejong University, Seoul, Republic of Korea
[19] Department of Physics, University of Oslo, Oslo, Norway
[20] Department of Physics and Technology, University of Bergen, Bergen, Norway
[21] Dipartimento di Fisica dell'Università 'La Sapienza' and Sezione INFN, Rome, Italy
[22] Dipartimento di Fisica dell'Università and Sezione INFN, Cagliari, Italy
[23] Dipartimento di Fisica dell'Università and Sezione INFN, Trieste, Italy
[24] Dipartimento di Fisica dell'Università and Sezione INFN, Turin, Italy
[25] Dipartimento di Fisica e Astronomia dell'Università and Sezione INFN, Bologna, Italy
[26] Dipartimento di Fisica e Astronomia dell'Università and Sezione INFN, Catania, Italy
[27] Dipartimento di Fisica e Astronomia dell'Università and Sezione INFN, Padova, Italy
[28] Dipartimento di Fisica 'E.R. Caianiello' dell'Università and Gruppo Collegato INFN, Salerno, Italy
[29] Dipartimento DISAT del Politecnico and Sezione INFN, Turin, Italy
[30] Dipartimento di Scienze e Innovazione Tecnologica dell'Università del Piemonte Orientale and INFN Sezione di Torino, Alessandria, Italy
[31] Dipartimento Interateneo di Fisica 'M. Merlin' and Sezione INFN, Bari, Italy
[32] Division of Experimental High Energy Physics, University of Lund, Lund, Sweden
[33] European Organization for Nuclear Research (CERN), Geneva, Switzerland
[34] Excellence Cluster Universe, Technische Universität München, Munich, Germany
[35] Faculty of Engineering, Bergen University College, Bergen, Norway
[36] Faculty of Mathematics, Physics and Informatics, Comenius University, Bratislava, Slovakia
[37] Faculty of Nuclear Sciences and Physical Engineering, Czech Technical University in Prague, Prague, Czech Republic
[38] Faculty of Science, P.J. Šafárik University, Košice, Slovakia
[39] Faculty of Technology, Buskerud and Vestfold University College, Tonsberg, Norway
[40] Frankfurt Institute for Advanced Studies, Johann Wolfgang Goethe-Universität Frankfurt, Frankfurt, Germany
[41] Gangneung-Wonju National University, Gangneung, Republic of Korea
[42] Gauhati University, Department of Physics, Guwahati, India
[43] Helmholtz-Institut für Strahlen- und Kernphysik, Rheinische Friedrich-Wilhelms-Universität Bonn, Bonn, Germany
[44] Helsinki Institute of Physics (HIP), Helsinki, Finland
[45] Hiroshima University, Hiroshima, Japan
[46] Indian Institute of Technology Bombay (IIT), Mumbai, India
[47] Indian Institute of Technology Indore, Indore, India
[48] Indonesian Institute of Sciences, Jakarta, Indonesia
[49] INFN, Laboratori Nazionali di Frascati, Frascati, Italy
[50] INFN, Laboratori Nazionali di Legnaro, Legnaro, Italy
[51] INFN, Sezione di Bari, Bari, Italy
[52] INFN, Sezione di Bologna, Bologna, Italy
[53] INFN, Sezione di Cagliari, Cagliari, Italy
[54] INFN, Sezione di Catania, Catania, Italy
[55] INFN, Sezione di Padova, Padova, Italy
[56] INFN, Sezione di Roma, Rome, Italy
[57] INFN, Sezione di Torino, Turin, Italy
[58] INFN, Sezione di Trieste, Trieste, Italy
[59] Inha University, Incheon, Republic of Korea
[60] Institut de Physique Nucléaire d'Orsay (IPNO), Université Paris-Sud, CNRS-IN2P3, Orsay, France
[61] Institute for Nuclear Research, Academy of Sciences, Moscow, Russia
[62] Institute for Subatomic Physics of Utrecht University, Utrecht, Netherlands
[63] Institute for Theoretical and Experimental Physics, Moscow, Russia
[64] Institute of Experimental Physics, Slovak Academy of Sciences, Košice, Slovakia
[65] Institute of Physics, Academy of Sciences of the Czech Republic, Prague, Czech Republic
[66] Institute of Physics, Bhubaneswar, India
[67] Institute of Space Science (ISS), Bucharest, Romania
[68] Institut für Informatik, Johann Wolfgang Goethe-Universität Frankfurt, Frankfurt, Germany
[69] Institut für Kernphysik, Johann Wolfgang Goethe-Universität Frankfurt, Frankfurt, Germany
[70] Institut für Kernphysik, Westfälische Wilhelms-Universität Münster, Münster, Germany
[71] Instituto de Ciencias Nucleares, Universidad Nacional Autónoma de México, Mexico City, Mexico
[72] Instituto de Física, Universidade Federal do Rio Grande do Sul (UFRGS), Porto Alegre, Brazil
[73] Instituto de Física, Universidad Nacional Autónoma de México, Mexico City, Mexico
[74] IRFU, CEA, Université Paris-Saclay, Saclay, France
[75] iThemba LABS, National Research Foundation, Somerset West, South Africa

[76] Joint Institute for Nuclear Research (JINR), Dubna, Russia
[77] Konkuk University, Seoul, Republic of Korea
[78] Korea Institute of Science and Technology Information, Daejeon, Republic of Korea
[79] KTO Karatay University, Konya, Turkey
[80] Laboratoire de Physique Subatomique et de Cosmologie, Université Grenoble-Alpes, CNRS-IN2P3, Grenoble, France
[81] Lawrence Berkeley National Laboratory, Berkeley, CA, United States
[82] Moscow Engineering Physics Institute, Moscow, Russia
[83] Nagasaki Institute of Applied Science, Nagasaki, Japan
[84] National and Kapodistrian University of Athens, Physics Department, Athens, Greece
[85] National Centre for Nuclear Studies, Warsaw, Poland
[86] National Institute for Physics and Nuclear Engineering, Bucharest, Romania
[87] National Institute of Science Education and Research, HBNI, Jatni, India
[88] National Nuclear Research Center, Baku, Azerbaijan
[89] National Research Centre Kurchatov Institute, Moscow, Russia
[90] Niels Bohr Institute, University of Copenhagen, Copenhagen, Denmark
[91] Nikhef, Nationaal instituut voor subatomaire fysica, Amsterdam, Netherlands
[92] Nuclear Physics Group, STFC Daresbury Laboratory, Daresbury, United Kingdom
[93] Nuclear Physics Institute, Academy of Sciences of the Czech Republic, Řež u Prahy, Czech Republic
[94] Oak Ridge National Laboratory, Oak Ridge, TN, United States
[95] Petersburg Nuclear Physics Institute, Gatchina, Russia
[96] Physics Department, Creighton University, Omaha, NE, United States
[97] Physics Department, Faculty of Science, University of Zagreb, Zagreb, Croatia
[98] Physics Department, Panjab University, Chandigarh, India
[99] Physics Department, University of Cape Town, Cape Town, South Africa
[100] Physics Department, University of Jammu, Jammu, India
[101] Physics Department, University of Rajasthan, Jaipur, India
[102] Physikalisches Institut, Eberhard Karls Universität Tübingen, Tübingen, Germany
[103] Physikalisches Institut, Ruprecht-Karls-Universität Heidelberg, Heidelberg, Germany
[104] Physik Department, Technische Universität München, Munich, Germany
[105] Purdue University, West Lafayette, IN, United States
[106] Research Division and ExtreMe Matter Institute EMMI, GSI Helmholtzzentrum für Schwerionenforschung GmbH, Darmstadt, Germany
[107] Rudjer Bošković Institute, Zagreb, Croatia
[108] Russian Federal Nuclear Center (VNIIEF), Sarov, Russia
[109] Saha Institute of Nuclear Physics, Kolkata, India
[110] School of Physics and Astronomy, University of Birmingham, Birmingham, United Kingdom
[111] Sección Física, Departamento de Ciencias, Pontificia Universidad Católica del Perú, Lima, Peru
[112] SSC IHEP of NRC Kurchatov institute, Protvino, Russia
[113] Stefan Meyer Institut für Subatomare Physik (SMI), Vienna, Austria
[114] SUBATECH, IMT Atlantique, Université de Nantes, CNRS-IN2P3, Nantes, France
[115] Suranaree University of Technology, Nakhon Ratchasima, Thailand
[116] Technical University of Košice, Košice, Slovakia
[117] Technical University of Split FESB, Split, Croatia
[118] The Henryk Niewodniczanski Institute of Nuclear Physics, Polish Academy of Sciences, Cracow, Poland
[119] The University of Texas at Austin, Physics Department, Austin, TX, United States
[120] Universidad Autónoma de Sinaloa, Culiacán, Mexico
[121] Universidade de São Paulo (USP), São Paulo, Brazil
[122] Universidade Estadual de Campinas (UNICAMP), Campinas, Brazil
[123] Universidade Federal do ABC, Santo Andre, Brazil
[124] University of Houston, Houston, TX, United States
[125] University of Jyväskylä, Jyväskylä, Finland
[126] University of Liverpool, Liverpool, United Kingdom
[127] University of Tennessee, Knoxville, TN, United States
[128] University of the Witwatersrand, Johannesburg, South Africa
[129] University of Tokyo, Tokyo, Japan
[130] University of Tsukuba, Tsukuba, Japan
[131] Université Clermont Auvergne, CNRS/IN2P3, LPC, Clermont-Ferrand, France
[132] Université de Lyon, Université Lyon 1, CNRS/IN2P3, IPN-Lyon, Villeurbanne, Lyon, France
[133] Université de Strasbourg, CNRS, IPHC UMR 7178, F-67000 Strasbourg, France
[134] Università degli Studi di Pavia, Pavia, Italy
[135] Università di Brescia, Brescia, Italy
[136] V. Fock Institute for Physics, St. Petersburg State University, St. Petersburg, Russia
[137] Variable Energy Cyclotron Centre, Kolkata, India
[138] Warsaw University of Technology, Warsaw, Poland
[139] Wayne State University, Detroit, MI, United States
[140] Wigner Research Centre for Physics, Hungarian Academy of Sciences, Budapest, Hungary
[141] Yale University, New Haven, CT, United States
[142] Yonsei University, Seoul, Republic of Korea
[143] Zentrum für Technologietransfer und Telekommunikation (ZTT), Fachhochschule Worms, Worms, Germany

[i] Deceased.
[ii] Dipartimento DET del Politecnico di Torino, Turin, Italy.
[iii] Georgia State University, Atlanta, Georgia, United States.
[iv] M.V. Lomonosov Moscow State University, D.V. Skobeltsyn Institute of Nuclear, Physics, Moscow, Russia.
[v] Department of Applied Physics, Aligarh Muslim University, Aligarh, India.
[vi] Institute of Theoretical Physics, University of Wroclaw, Poland.